Needle vs. Powder Imaging Plate for Computer Radiography: Image Quality Measurement and Model Calculation

Peter Willems, Paul J. R. Leblans and Bert M.F. De Winter, Research & Development of Materials, Technical Imaging, Agfa-Gevaert N.V., Belgium

Abstract

Computed radiography (CR) is a digital radiography technology in which a storage phosphor plate is used to store a latent X-ray image. The plate is exposed in a light-tight cassette and then read out in a scanner to create the digital image. Conventionally, CR powder imaging plates (PIP) are used based on $BaFBr_{1-x}I_x$:Eu^{2+} phosphor. The active layer consists of phosphor microcrystals in a polymer binder. A needle imaging plate (NIP), created by of vapor deposition of needle-shaped phosphor crystals, leads to better image quality because thicker phosphor layers, having higher X-ray absorption can be used. $BaFBr_{1-x}I_x$:Eu^{2+} is an excellent storage phosphor. It decomposes upon vaporization, however. For that reason, it is impossible to vapor deposit $BaFBr_{1-x}I_x$:Eu^{2+} needle crystals. At Agfa an excellent new storage phosphor, CsBr:Eu^{2+}, was discovered. Since CsBr melts congruently, it allows thermal vapor deposition and production of NIP's. Measurements demonstrate that CsBr:Eu^{2+} NIP's allow to double CR image quality (DQE). A linear-systems approach is used to model signal and noise transfer in a CR system using PIP or NIP. The transfers are described by cascading transfer relationships for each process. The calculated image quality (DQE) is in good agreement with measurement for the PIP system. The model overestimates the NIP system DQE at high spatial frequencies. An overestimation of the system gain may be the reason.

Introduction

In CR storage phosphors, free electrons and holes released by X-ray quanta are trapped in storage centers, to generate a latent image. In the read-out process in the scanner, the trapped electrons are stimulated with red light to give rise to blue luminescence signal, which is transformed in an electronic signal by a light sensor and digitized.[1]

Today, storage phosphors of the $BaFBr_{1-x}I_x$:Eu^{2+} family are used in commercial CR systems. $BaFBr_{1-x}I_x$:Eu^{2+} is used in the plates of Agfa, Fuji, Kodak and Konica. It is an excellent storage phosphor with a high storage capacity and a relatively high specific X-ray absorption. Since $BaFBr_{1-x}I_x$:Eu^{2+} does not melt congruently it decomposes upon vaporization, which makes it unfit for NIP manufacturing.

Agfa discovered an excellent new storage phosphor, CsBr:Eu^{2+}, with a chemical composition and density of 4.5 g/cm^3 that lead to a specific X-ray absorption that is similar to that of $BaFBr_{1-x}I_x$:Eu^{2+}.[2] NIP leads to better image quality than PIP for two reasons. The needles provide strong forward light scattering, thereby strongly reducing light spread in lateral direction in the phosphor layer. As a consequence, image sharpness is much higher at equal thickness. Also, no binder is present, which implies a higher phosphor packing density and, thus, a higher X-ray absorption. Image quality of a CR system with the CsBr:Eu^{2+} NIP was measured and compared to the image quality of a state-of-the-art CR system with the $BaFBr_{1-x}I_x$:Eu^{2+} PIP. A computer program based on an image quality model for CR systems has been developed. Image quality model predictions are compared to measurement results.

DQE as Imaging System Quality Measure

The DQE can be considered as the figure of merit of an imaging system. It is defined as:

$$DQE = SNR_{out}^{2} / SNR_{in}^{2} \qquad (1)$$

where SNR_{in} is the signal-to-noise ratio of the incoming X-ray image and SNR_{out} is the signal-to-noise ratio of the image produced by the imaging system. In other words the DQE is a measure of image quality preservation by the imaging system. It varies between 0 and 100%. In the frequency-dependent DQE the effect of resolution loss is accounted for as well.

Experimental

CR Systems

The reference PIP system, is a commercial system reported on in Ref. [3] as system no. 2. It is a conventional flying-spot scanner, using the commercial Agfa MD30.0 $BaFBr_{1-x}I_x$:Eu^{2+} PIP.

The NIP was scanned with a scanner, based on the new scan-head technology.[4] A scan-head, consisting of a diode array with a cylindrical lens scans the phosphor layer, stimulating the NIP with focussed red laser light in a line-wise fashion. The blue luminescence light generated is focussed by a lens system on a CCD line sensor with 50 μ resolution. Through 2x2 binning, 100 mu pixels are produced. The table below lists the PIP and NIP system characteristics.

Table 1: CR System Characteristics

Plate	PIP	NIP
Phosphor	$BaFBr_{1-x}I_x$:Eu^{2+}	CsBr:Eu^{2+}
Coating weight (mg/cm^2)	85	169
Thickness (mu)	240	470
Scanner type	Flying-spot	Scan-head
Scanning method	Pixel wise	Line wise
Pixel size (mu)	114	100
Light guide	Fiber optic	Lens system
Detector	PMT	CCD array

Measurement Procedures and Exposure Conditions

The PIP CR system technical image quality was determined in Ref. [3] according to the methods of the IEC 62220 standard. For the NIP CR system the MTF and the noise power spectrum were measured in close approximation to the methods described in the standard. Differences were: No use of additional diaphragms “B2” and “B3”; use of a 100 mm x 50 mm x 2 mm tungsten edge instead of the specified edge; use of 1 million independent pixels for normalized noise power (NNP) calculation instead of 4 million; use of a block of 128 x128 pixels instead of 256 x 256 pixels for NNP calculation. The X-ray spectrum used in the measurements corresponded to the RQA 5 radiation quality, with an X-ray tube voltage of 70 kVp, an internal Al filter of 2.5 mm and an external Al filter of 21 mm. The resulting Al half-value layer was ca. 7.1 mm. The normalized noise power was determined at a dose of ca. 0.8 muGy, and the MTF at a dose of ca. 8.0 muGy. The dose was measured with a solid state dosimeter prior to the exposure (Unfors 567 L). As X-ray source a GMM medical X-ray device with focal spot size of 0.6 mm was used.

Measurement Analysis

DQE Calculation

The 2-dimensional frequency-dependent detective quantum efficiency DQE(u,v) is given by:

$$DQE(u,v). = MTF^2(u,v).W_{in}(u,v)/W_{out}(u,v) \qquad (2)$$

where MTF is the presampled modulation transfer function of the imaging device, W_{out} the noise power spectrum of the flat-field image made with the X-ray imaging device and W_{in} the noise power spectrum of the incoming X-radiation at the detector, i.e. phosphor plate surface. The input noise power spectrum is equal to the incoming X-ray quantum fluence and is constant for all spatial frequencies (white noise). For the RQA 5 exposure conditions used, the incoming X-ray quantum fluence was taken to be 30,174 $mm^{-2}muGy^{-1}$.

The DQE in the slow-scan direction was used for comparison between the systems and for comparison with model calculations.

Model Description

General

The software developed to calculate a digital X-ray system DQE has different sections. Section 1 generates the X-ray spectrum produced by the X-ray source.

Section 2 generates the X-ray spectrum after transmission through an external filter, usually present in an X-ray imaging system. The output of section 2 is the X-ray spectrum incident on the phosphor plate.

In section 3 the generation of light by the X-ray quanta and the optical stimulation in the scanner is calculated.

The final section deals with the photon detection process in the scanner. For CR systems and in the medical, general radiography dose range screen-structure noise and electronic noise can be neglected. Hence, only quantum noise is considered in the model calculation.

Sections 1 and 2: X-ray Spectrum Generation

The X-ray spectra are calculated with the equations proposed by Boone et al..[5] Measured spectra have been parameterized using polynomial interpolation of the spectral data. The attenuation of arbitrary internal filtration on the spectra is calculated using the energy-dependent Lambert-Beer law. The attenuation of an arbitrary external filter package is calculated in the same way. In section 2 it is also possible to calculate the (air Kerma) absorption of the filter package.

Section 3: Interaction of X-rays with Phosphor Plate

Section 3 covers the interaction of X-ray quanta with the phosphor layer and the generation of light in the stimulation process. The linear-systems approach[6] is used to describe both signal and noise transfer in the system. The link is made to metrics of image quality and system performance including the modulation transfer function (MTF), noise power spectrum (NPS) and detective quantum efficiency (DQE). The cascaded systems approach represents the imaging system as a series of discrete stages, where each stage represents a process which affects either the mean number of image carriers, a gain stage, or the spatial distribution of the image carriers, a spatial spreading stage. Each of these processes has distinct signal and noise transfer characteristics.

First, the interaction of X-rays with the plate is modeled. The spectrum of the X-rays that deposit energy in the screen is calculated using the energy dependent law of Lambert-Beer and using the mass-energy absorption coefficients of the phosphor material. Since the plate response is not homogeneous, it is split up in a number of virtual layers in the thickness direction and the energy deposited in each layer is calculated. The energy needed to create a storage center in the storage phosphor being known, this allows to calculate the number of storage centers being created in each layer.

Next, stimulation of the phosphor plate by the scanner in the read-out phase is modeled. A stimulation efficiency is assumed for each virtual layer of the phosphor screen, giving the fraction of storage centers that will give rise to an optical photon. It is assumed that the stimulation efficiency in the top layer is higher than the stimulation efficiency in the bottom layer. For the intermediate layers, the stimulation efficiency is obtained by linear interpolation. Photons generated in the stimulation process have a certain escape efficiency towards the scanner optics. Again, each virtual phosphor plate layer is assumed to have a different escape efficiency, the escape efficiency from the top layer being higher than the escape efficiency from the bottom layer. The stimulation and light emission stages give rise to spatial spreading of the signal, caused by lateral light diffusion. Therefore, an MTF is connected to these stages. In our model, the MTF of the stimulation and emission stages is described by a Lorentzian, which is different for each virtual phosphor plate layer:

$$MTF(u) = [1 + (u/H)^2]^{-1} \qquad (3)$$

The Lorentz factor H is assumed to be higher for the top than for the bottom layer of the plate. The H values for the intermediate layers are calculated by linear interpolation. The noise transfer of these 3 stages is calculated using the cascaded systems approach. The NPS is calculated for every virtual layer using the input parameters for the individual layers as described. The total NPS is calculated by summing the NPS of the individual layers.

The system MTF at this stage is calculated as the weighted average of the virtual layers' MTF, the weighing factors being the relative contributions of the layer to the signal. The weighing factor, therefore, depends on the X-ray absorption and on the stimulation and escape efficiencies of the virtual layer.

The DQE at this stage is calculated as:

$$DQE(u) = q_0.G^2.MTF(u)^2/NPS(u) \qquad (4)$$

where q_0 is the mean number of quanta incident on the screen and G is the gain of the phosphor plate, i.e. the number of photons per incident X-ray quantum.

Section 4: Conversion of Photons to Photoelectrons

The signal conversion stage deals with the transmission of photons to the detector by the scanner optics, with the passage through the filter for stopping the stimulation light and with the conversion to photoelectrons. The total system gain is calculated as the gain of the previous stage, multiplied by the transmission efficiency of the light guide, the transmission of the filter and the quantum efficiency of the light detector.

The noise transfer is again calculated using the cascaded systems approach.

The presampling MTF represents the deterministic spreading of the photons by the pixel aperture. It is considered as deterministic since each integrated photon is conceptually redistributed to a single point (the pixel center) at which it will be counted. The presampling MTF is modeled with a sinc function. The total system MTF is calculated as the MTF of the previous stage, multiplied by the sinc function.

Model Calculation

Sections 1 and 2: X-ray Spectrum Generation

An X-ray spectrum corresponding to the RQA 5 Al half-value layer of 7.1 mm was generated. To obtain this HVL, the W-generator X-ray source high voltage had to be set at 73 kVp for the combination with the internal 2.5 mm Al filter and the external 21 mm Al filter.

Section 3: Interaction of X-rays with PIP and NIP

The X-ray absorption was calculated for a BaFBr phosphor layer with an equivalent thickness (at 100% fill factor) of 170 mu, which corresponds to the plate coating weight of 85 mg/cm^2. The CsBr phosphor layer was assumed to have an equivalent thickness of 376 mu, corresponding to the plate coating weight of 169 mg/cm^2. The average energy of the absorbed X-ray quanta was calculated to be ca. 52 keV for both PIP and NIP. The energy needed to generate a storage center in BaFBr:Eu^{2+} being 100 eV, the number of storage centers generated per absorbed X-ray quantum in PIP is 520. It was assumed that the energy needed to generate a storage center in CsBr:Eu^{2+} is 100 eV as well. The phosphor plates were divided in 15 virtual layers in the plate thickness direction. The average stimulation efficiency in the PIP CR system being 60%, it was assumed that 70% of the storage centers in the top layer gave rise to an optical photon, whereas only 50% of the storage centers in the bottom layer was stimulated. Similarly, the photon escape efficiency was estimated to be 70% for the top layer and 50% for the bottom layer. The average stimulation efficiency in the NIP CR system being ca. 75%, it was assumed that 80% of the storage centers in the top layer gave rise to an optical photon, whereas 70% of the storage centers in the bottom layer was stimulated. Similarly, the photon escape efficiency was estimated to be 80% for the top layer and 70% for the bottom layer. The MTF Lorentzians were adjusted to obtain a good fit of the measured systems' MTF.

Section 4: Conversion of Photons to Photoelectrons

In the PIP scanner, the light emitted by the phosphor screen is guided to a photomultiplier tube by a fiber optic having a coupling efficiency of 35%. The filter in front of the PMT, has a transmission of 75% and the PMT has a quantum efficiency of 25%. In the NIP line-scanner, the light is guided to a CCD array, for detection by a lens system having a coupling efficiency of 10%. The filter also has a transmission efficiency of 75% and the CCD detector has a quantum efficiency of 65%. Therefore, the NIP scanner has a ca. 25% lower photon detection efficiency than the PIP scanner. Table 3 summarizes the parameters used for both systems.

Table 2: Model Parameters for PIP and NIP System DQE Calculation

System	PIP	NIP
Phosphor matrix material	BaFBr	CsBr
Phosphor layer thickness (mu)	170	376
# virtual plate layers	15	15
Storage center generation energy (eV)	100	100
Stimulation efficiency (X-ray side) (%)	70	80
Stimulation efficiency (bottom) (%)	50	70
Escape efficiency (X-ray side) (%)	70	80
Escape efficiency (bottom) (%)	50	70
MTF Lorentzian (X-ray side)	1.5	1.9
MTF Lorentzian (bottom)	0.5	1.2
Coupling efficiency optics (%)	35	10
Filter transmission (%)	75	75
Detector quantum efficiency (%)	25	65
Pixel aperture (mu)	114	100

Results

MTF

Figure 1 shows the measured and calculated MTF. It is striking that the NIP system leads to a clearly higher sharpness than the PIP system although the NIP has a much higher coating weight. This is a result of the different light scattering behavior in the 2 types of plate. In PIP unsharpness is caused by scattering of the stimulating light beam. Due to the particulate nature of the phosphor, the light is scattered in all directions and, therefore, equally in the lateral and the depth direction. The needle shape of the phosphor crystals in NIP results in a scattering process that is much stronger in the forward direction than in the lateral direction. Hence, the halo in NIP is smaller than in PIP notwithstanding the much higher coating weight. Also, light penetrates much deeper into a NIP layer than in a PIP layer, resulting in a higher stimulation and escape efficiency. The experimental MTF curves can be fitted very well with the model using a different Lorentzian function to describe the MTF of the virtual plate layers, obtained by linear interpolation of the Lorentzians for top - and bottom layers.

DQE

Figure 2 shows the measured and calculated DQE curves for both systems. Thanks to the much higher X-ray absorption of the NIP plate, its excellent optical transparency and its higher MTF, the NIP CR system has a much higher DQE.

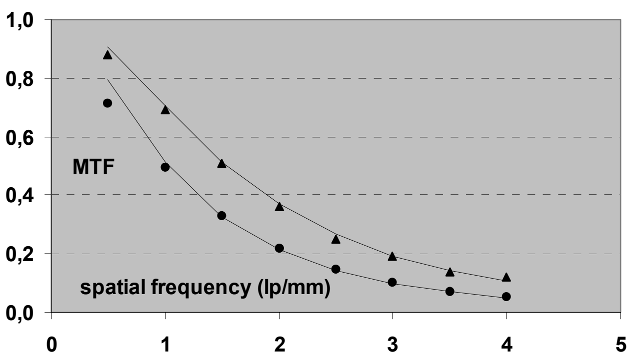

Figure 1. Measured PIP (•) and NIP (▲) CR systems' MTF and fitted values (lines)

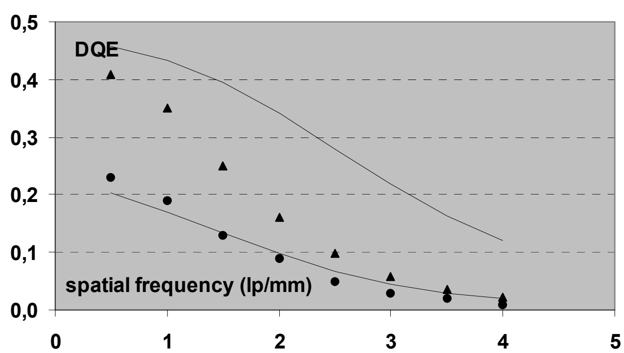

Figure 2. Measured PIP (•) and NIP (▲) CR systems' DQE and calculated values (lines)

As shown in Fig. 3 the DQE ratio (NIP-to-PIP) is ca. 2 over the entire spatial frequency range. As indicated in Ref. 7 the much higher DQE of the NIP CR system results in a superior performance of the system in observer performance studies. There is good correspondence between the measured and calculated DQE values for the PIP system.

The model predicts relatively well the low-spatial frequency NIP system DQE. At higher spatial frequencies, the model strongly overestimates the DQE. To obtain good correspondence between calculated and measured image quality for the NIP system a 4 times lower system gain has to be used in the model calculation (Fig. 4). It is not clear whether the NIP system gain is, indeed, lower than assumed. If so, a significant further improvement of CR image quality is possible by a system gain increase. Further research is ongoing to explain the discrepancy between measured and calculated image quality.

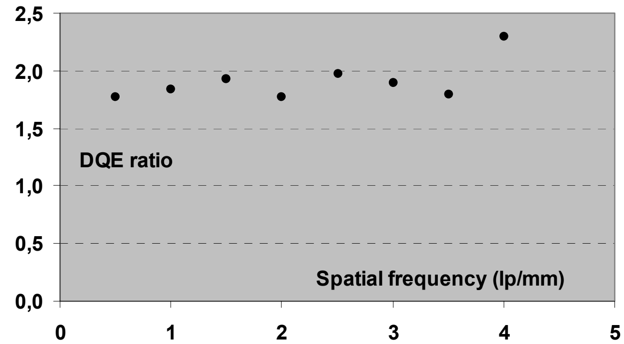

Figure 3. Ratio of NIP system-to-PIP system DQE

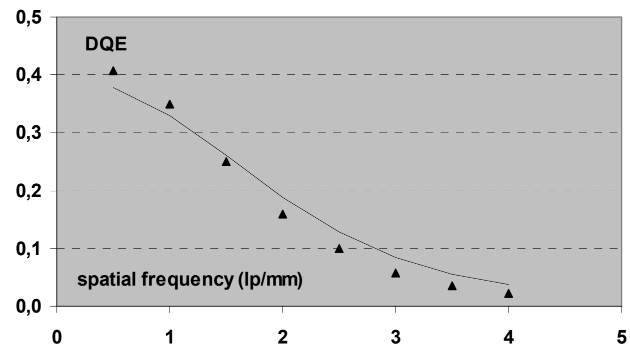

Figure 4. Measured (▲) and calculated DQE values (lines) for the NIP system, assuming a 4x lower system gain

References

1. K. Takabahashi, K. Kohda, Y. Shibahara, J. Electrochem. Soc.: Solid State Science and Technology 132, 1492 (1985).
2. P.J.R. Leblans, L. Struye, P. Willems, Proc. of SPIE, 4320, 59 (2001).
3. H. Illers, E. Buhr, D. Bergmann, C. Hoeschen, Proc. of SPIE, Vol. 5, 22, 177 (2004).
4. R. Schaetzing, RSNA Course in Diagnostic Radiology Physics, 7 (2003).
5. J. M.Boone, T.R.Fewell, R. J.Jennings, Medical Physics 24 , 12 (1997).
6. J. H.Siewerdsen, Dissertation submitted in partial fulfullment of the requirements for the degree of Ph D (Physiscs) at the Univ. of Michigan (1998).
7. J. Frankenberger, S. Mair, C. Herrmann, J. Lamotte, R. Fasbender, Proc. of SPIE (2005).

Author Biography

Paul Leblans received his Ph.D. from Antwerp University in 1986. He worked at DSM, The Netherlands as polymer rheologist from 1986 to 1990. In this period he lectured in The Netherlands at Technical Highschool, Heerlen, and at the Technical University, Eindhoven. In 1990 he joined Agfa-Gevaert, to work on storage phosphors. Today, he is research project manager in digital radiography detectors. His activities include storage phosphor research; phosphor screen development and medical systems' image quality modeling.